CORRECTIONS OF A CAVITY SHAPE DUE TO ETCHING, COOLING DOWN, AND TUNING*

Valery Shemelin†
Cornell Laboratory for Accelerator-based Sciences and Education (CLASSE), Ithaca, NY 14853

Abstract

Corrections of shape needed for an SRF cavity after fabrication are presented in a convenient form with a possibility to take into account different technological procedures, such as etching, cooling down and pre- loading.

INTRODUCTION

Optimization of the cavity shape consists mainly in a search of the final shape in a cooled-down state after all the technological procedures including etching and preliminary loading. The preloading is needed with a goal to get rid of backlash when the cavity is being tuned to the work frequency. So, the drawing dimensions should differ from these final dimensions if we want to end up with the calculated dimensions. Moreover, it is a question, whether these dimensions are dimensions of elliptic arcs routinely used for description of the cavity shape. It would be useful to find a convenient form of taking into account all of these changes of shape. It is even more important to keep the designed dimensions if the cavity is optimized for minimal BBU parameter, because the higher order modes responsible for beam break up - are even more sensitive to distortion of dimensions than the fundamental mode.

MATRIX DESCRIPTION OF THE CAVITY SHAPE

If we look at any multicell cavity shape, we can note that it can be presented as a chain of elliptic arcs connected with straight segments tangent to them, Figure 1. So, a full description of the final dimensions of such a cavity excluding the lengths of end pipes can be presented as:

$$\text{dim\_}f = \begin{pmatrix} x1 & x2 & \cdots & x\text{n} \\ y1 & y2 & \cdots & y\text{n} \\ a1 & a2 & \cdots & a\text{n} \\ b1 & b2 & \cdots & b\text{n} \end{pmatrix}$$

"Final" means that the cavity is cooled down after all technological preparations which can change the dimensions (etching and, possibly, tumbling), and preloading. In the first line of the matrix are longitudinal coordinates of the centers of the elliptic arcs, in the second line – the radial coordinates of the centers, in the third and fourth – longitudinal and radial half-axes of the ellipses, respectively.

* Supported by NSF award DMR-0807731
† vs65@cornell.edu

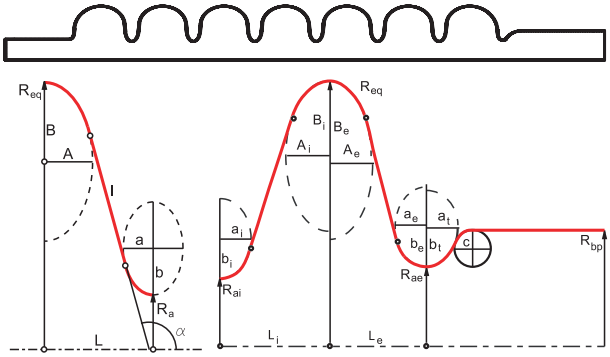

Figure 1: A multicell cavity (upper picture) and its presentation as a chain of elliptic arcs connected with straight segments: inner half-cell and end cell (lower pictures). End cells can have an additional iris: compare the right and left ends.

If shrinkage only due to Nb thermal contraction from 293 K to 0 K is considered, the starting dimensions of the cavity should be bigger by the factor of $1+kT = 1+1.43\cdot 10^{-3}$ [1]:

$$\text{dim\_}s = \text{dim\_}f \cdot (1 + kT).$$

If etching only is taken into account, then

$$\text{dim\_}s = \text{dim\_}f - \text{Etch},$$

where the matrix Etch looks like

$$\text{Etch} = \begin{pmatrix} 0 & 0 & \cdots & 0 \\ 0 & 0 & \cdots & 0 \\ ex1 & ex & \cdots & ex\text{n} \\ ey & ey2 & \cdots & ey\text{n} \end{pmatrix},$$

where positive values in the third and fourth rows correspond to concave surfaces (equatorial ellipses) and negative values of ex or ey are for decreasing half-axes (irises). Here we can take into account different values of etching for equatorial and iris regions if they are known from experiment (different ellipses = different columns) and even for lower and upper parts of the ellipses (for different axes = different rows). Now, if only compression (or stretching) of the cavity should be accounted, we can write

$$\text{dim\_}s = \text{dim\_}f - \text{P} \cdot \Delta L,$$

where P is the matrix of "pliability":

$$\mathrm{P} = \begin{pmatrix} px1 & px2^* & \cdots & px\mathrm{n}^* \\ py1 & py2 & \cdots & py\mathrm{n} \\ pa1 & pa2 & \cdots & pa\mathrm{n} \\ pb1 & pb2 & \cdots & pb\mathrm{n} \end{pmatrix},$$

$px1$, $px2$, ... and so on are coefficients in the relations: $\Delta x1 = px1 \cdot \Delta L$, $\Delta y1 = py1 \cdot \Delta L$, ... and so on. ΔL is total compression of the cavity. Asterisks designate the cumulative values:
$px2^* = px1 + px2$, $px3^* = px2^* + px3$, ... and so on.

All the corrections are small, so we take into account the first order only and unite them in the final formula:

$$\mathrm{dim\_}s = \mathrm{dim\_}f \cdot (1 + kT) - \mathrm{Etch} - \mathrm{P} \cdot \Delta L.$$

CONSERVATION OF THE ELLIPTIC SHAPE

Because of small changes of dimensions, one can expect that the deviation from the original shape will not lead to non-elliptical shapes but it is better to analyze the actual simulation data [2] at least for the deformation used for cavity tuning.

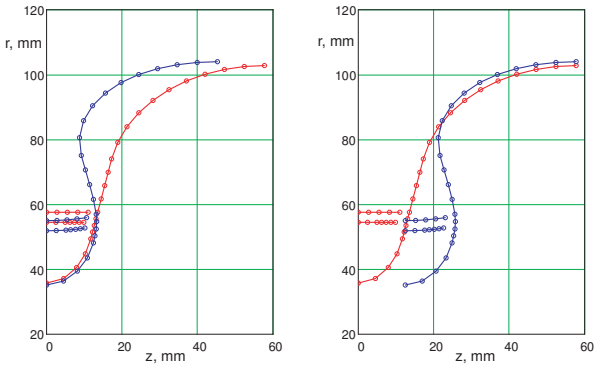

Figure 2: Deformation of the half-cell with stiffening rings. Outer surface of the cavity is not shown.

Results of the simulation are presented in Figure 2. In this figure the deformation of $\Delta L = 13$ micrometers is magnified 1000 times. Keeping the left-most or the right-most right point of the half-cell at place (the left or the right picture) one can see that deformations of the equatorial and iris regions are relatively small and deformation is mostly at the cost of tilting the straight line area. It is seen that the stiffening ring also deforms. The outer surface of the cavity is not shown. Thickness both of the ring and of the cavity wall is 3 mm. After deformation the elliptic shape of the equatorial and the iris area is kept, Figure 3. Moreover, the straight segment is tangent to the arcs as before with a good accuracy. One can note also that tuning to the desired frequency occurs not because of change of the equatorial radius as is stated in [3] but because of change of the wall slope angle and of the capacitance due to decrease of the distance between irises.

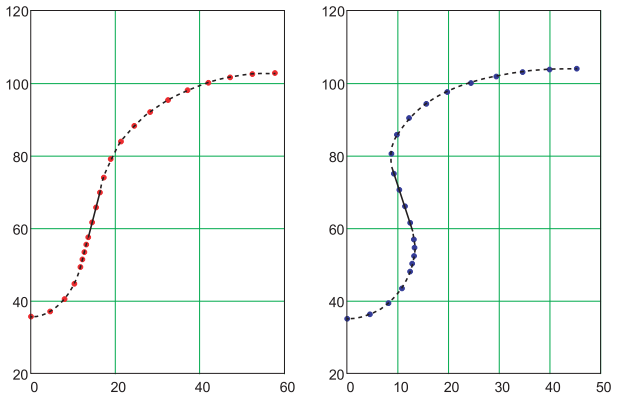

Figure 3: After deformation the shape keeps elliptic arcs with a straight segment between them.

Table 1: Coefficients of the P matrix for the inner cell, designations from Fig. 1 (lower left) are used for Fig. 3.

Iris Area		Equator Area	
$px1 = \Delta x/\Delta L$	0	$px2 = \Delta X/\Delta L$	1
$py1 = \Delta y/\Delta L$	0.047	$py2 = \Delta Y/\Delta L$	-1.013
$pa1 = \Delta a/\Delta L$	-0.077	$pA1 = \Delta A/\Delta L$	0.380
$pb1 = \Delta y/\Delta L$	0	$pB1 = \Delta Y/\Delta L$	0.919

For illustration, the relations between shortening of the cavity ΔL and changing of other dimensions (see designations for the inner cell in Fig. 1 on the lower left) for the Cornell ERL multicell cavity inner cell are presented in the Table 1.

In the case of the presented ERL inner cell the sensitivity to loading is 300 kHz/52 μm. The value of 300 kHz can be sufficient for preloading. Cooling down will change the dimensions up to 150 μm (equatorial radius), and etching is about 150 – 200 μm (sometimes light etching is used after the usual etching procedure). All these values are of the same order of magnitude but possibly the deformation from mechanical tuning can be neglected because it is smaller than the accuracy of fabrication (200 - 500 μm). However, in some cases, when no stiffening rings are used or higher preloading is implemented, this deformation can be bigger and should be accounted.

Consideration and correction of different deformations can be also useful for the right understanding of the position and properties of higher order modes.

USAGE OF THE MATRIX APPROACH TO THE ERL MULTICELL CAVITY

Dimensions of the ERL 7-cell cavity cells were optimized taking into account different constraints [4].The matrix of final dimensions (in mm) of this cavity can be presented in the form:

$$\text{dim\_}f = \left(\begin{array}{cccc|c} 318.54 & 354.42 & 354.42 & 412.42 & 0 \\ 19 & 56.95 & 60.30 & 62.35 & 67.31 \\ 36 & 11.27 & 12.49 & 41.51 & 41.35 \\ 36 & 20.95 & 24.30 & 40.53 & 35.57 \\ \hline 57.65 & 1104.25 & 1161.39 & 1161.39 & 1197.26 \\ 57.12 & 62.35 & 60.03 & 56.96 & 19 \\ 12.35 & 40.91 & 12.57 & 11.28 & 36 \\ 21.14 & 40.53 & 24.02 & 20.95 & 36 \end{array}\right).$$

We will not repeat in this matrix the inner half-cells dimensions 12 times with a constant shift in the first line and mirror reflections of the adjacent half-cells, so one only central half-cell is presented in the fifth and sixth columns. Conditionally, the origin z-coordinate here is taken equal to 0. The left and right end groups are described in the first and last four columns respectively. Both end groups have an additional iris like in Figure 1 lower right.

With regard to thermal contraction ($1.43 \cdot 10^{-3}$) and equal etching of all the surfaces by $\Delta = 150\,\mu m$ we have

$$\text{dim\_}s = \text{dim\_}f \cdot (1 + kT) - \text{Etch},$$

where

$$\text{Etch} = \left(\begin{array}{cccc|cc|cccc} 0 & 0 & 0 & 0 & 0 & 0 & 0 & 0 & 0 & 0 \\ 0 & 0 & 0 & 0 & 0 & 0 & 0 & 0 & 0 & 0 \\ -1 & 1 & 1 & -1 & -1 & 1 & -1 & 1 & 1 & -1 \\ -1 & 1 & 1 & -1 & -1 & 1 & -1 & 1 & 1 & -1 \end{array}\right) \cdot \Delta,$$

and starting dimensions for the designer drawings are:

$$\text{dim\_}s = \left(\begin{array}{cccc|c} 319.01 & 354.93 & 354.93 & 413.01 & 0 \\ 19.03 & 57.03 & 60.39 & 62.44 & 67.41 \\ 35.90 & 11.44 & 12.66 & 41.42 & 41.26 \\ 35.90 & 21.13 & 24.48 & 40.44 & 35.47 \\ \hline 57.74 & 1105.83 & 1163.05 & 1163.05 & 1198.97 \\ 57.20 & 62.44 & 60.12 & 57.04 & 19.03 \\ 12.52 & 40.82 & 12.74 & 11.44 & 35.90 \\ 21.32 & 40.44 & 24.21 & 21.13 & 35.90 \end{array}\right).$$

A small difference of the end irises outer elliptic arcs can be neglected because it is less than accuracy of production and the elliptic arc center radial coordinate can be taken as 57.03 mm for both irises. Besides, the initial radius of the beam pipe is 55 mm, and it should coincide with the sum of the end iris radius (now 35.90) and the position of its center (19.03). However, there is no necessity to strictly keep the circle radius of 36 mm or its center position as the final dimensions because this circle is chosen for multipactor preventing [5] and can be varied in a wide range. In this case we need only to correct the z-coordinates of the extreme circles. After all these corrections the matrix of **dimensions for the production drawings** can look like this:

$$\text{dim\_}s = \left(\begin{array}{cccc|c} 318.91 & 354.93 & 354.93 & 413.01 & 0 \\ 19 & 57.03 & 60.39 & 62.44 & 67.41 \\ 36 & 11.44 & 12.66 & 41.42 & 41.26 \\ 36 & 21.13 & 24.48 & 40.44 & 35.47 \\ \hline 57.74 & 1105.83 & 1163.05 & 1163.05 & 1199.07 \\ 57.20 & 62.44 & 60.12 & 57.03 & 19 \\ 12.52 & 40.82 & 12.74 & 11.44 & 36 \\ 21.32 & 40.44 & 24.21 & 21.13 & 36 \end{array}\right). \quad (1)$$

CORRECTION FOR MEASUREMENT CONDITIONS

The frequency of the central cell with the dimensions shown in the matrix (1) calculated by SLANS is $f_{calc} = 1299.655$ MHz. This is a frequency at room temperature ($T_{nc} = 293\ K$) but without regard for dielectric permittivity of air. ϵ of air depends on the atmospheric pressure p, humidity ϕ, and temperature T [6]:

$$\epsilon = 1 + 210 \cdot 10^{-6} \frac{p}{T} + \phi \frac{p_{sv}}{T} \left(\frac{10040}{T} - 0.30\right) \cdot 10^{-6}$$

Here p and p_{sv} are measured in mm Hg, T - Kelvin, ϕ – %. In this formula compared to the original one, the change is made from p_{air} to $p_{air} = p - p_{sv} \cdot \phi/100$, where p_{sv} is the water's vapour saturated pressure at the given temperature, so that the directly measured atmospheric pressure can be used. For p_{sv}, instead of an inconvenient table, I offer to use an approximation (from [7]):

$$\log p_{sv} = 7.45 \cdot \frac{t - 273}{T - 38.3} + 0.656,$$

which pretty good coincides with table data used in [3]. Instead of measuring every time parameters of atmosphere, one can measure one and the same *reference dumbbell* every time before starting the new measurements and take the correction from this measurements. Time to time this reference dumbbell should be checked using the ambient parameters, for the case it is deformed.

CONCLUSION

A convenient method to calculate corrections of the cavity shape from theoretical final dimensions to the drawing dimensions for mechanical workshop is presented. This matrix method can take into account changes of the cells shapes due to cooling down to cryogenic temperature, mechanical tuning, and chemical etching. Corrections of frequency due to atmospheric conditions are also analyzed.

REFERENCES

[1] "Brookhaven National Laboratory Selected Cryogenic Data Notebook", BNL, 10200-R, Vol. 1, IX-Q-1.

[2] Simulations with ANSYS were done by Sam Posen.

[3] F. Marhauser. JLab Cavity Fabrication Errors, Concequences and Lesson Learned. JLab-TN-10-021, 2010.

[4] N. Valles and M. Liepe. Seven-cell cavity optimization for Cornells energy recovery linac. In *Proc. of SRF2009,* Berlin, Germany.

[5] S. Belomestnykh and V. Shemelin. Multipacting-free transitions between cavities and beam-pipes. *Nucl. Instr. and Methods in Physics Research* A 595 (2008) 293 – 298.

[6] A. C. Strickland, RRB 1594, National Physical Laboratory, Dep. of Sci. and Ind. Research, 1942.

[7] Reference book on electromagnetic materials. Editor K.A. Andrianov. V. 1 of 2. Moscow – Leningrad, GEI, 1958.